Journal of Engineering and Applied Sciences 3 (6): 462-470, 2008
ISSN: 1816-949X

A New GCPW-Fed Fractal Printed Monopole Antenna Based on Tent Transformations for Modern Communication Systems

Jawad K. Ali and Adil H. Ahmad
Department of Electrical and Electronic Engineering, University of Technology,
P.O. Box 35239, Baghdad, Iraq

Abstract: In this study, a reduced size, low profile multiband printed GCPW-fed monopole antenna is presented as a candidate for use in multi-functions wireless communication systems. The proposed fractal antenna structure is based on the tent transformations. The self-similarity of the resulting monopole antenna substructures results in a multi-resonant behavior. To provide a wideband impedance matching and bandwidth enhancement to the antenna performance a grounded coplanar waveguide (GCPW) feed technique has been used. Theoretical performance of monopole antennas based on 1st and 2nd iterations of this fractal geometry has been calculated using a method of moments (MoM) based software, IE3D, from Zeland Software Inc. Results have shown that the proposed monopole antenna design possesses a multi-band resonant behavior with adequate radiation performance with VSWR $\leq$ 2 (return loss$\leq$-10 dB) throughout the resonating bands. An attempt has been carried out to correlate the proposed antenna dimensions with its resonant frequencies, to serve as an approximate aid in the initial design stage. This makes the presented antenna suitable for use in the modern multi-functions compact communication systems.

Key words: Fractal antenna, multi-band antenna, printed dipole antenna, IFS (iteration function system), GCPW feed

INTRODUCTION

The word fractal comes from Latin fractus, which means broken lines and Mandelbrot (Mandelbrot, 1983) first used it. Mandelbrot defined a fractal as a rough or fragmented geometric shape that can be subdivided in parts, each of which is (at least approximately) a reduced-size copy of the whole. Euclidean geometries are limited to points, lines, sheets and volumes and assigns an integer number to describe the dimension of each of these geometries; where the dimension of a point is zero and 1, 2 and 3 are the dimensions of the line, sheet and volume, respectively. Fractal geometry describes objects in nature by dimensions, which are not conditionally integer numbers as the Euclidean geometry implies. Euclidean geometries can be considered as special cases from the more general fractal geometries.

Fractals can be either random or deterministic. Most fractal objects found in nature are random, that have been produced randomly from a set of non-determined steps. Fractals that have been produced as a result of an iterative algorithm, generated by successive dilations and translations of an initial set, are deterministic.

Fractals are characterized by the self-similarity, the fractional dimension and space-filling properties. The

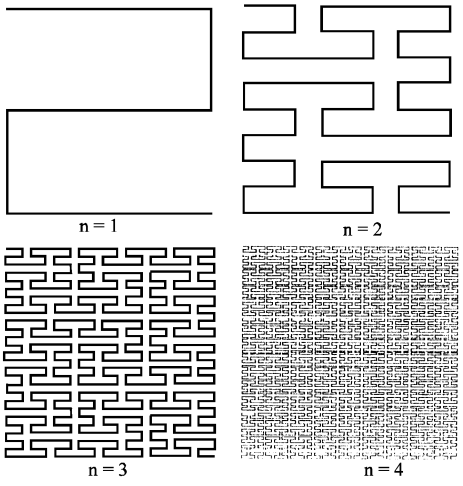

Fig. 1: The first four iteration levels to generate the Peano pre-fractal curve

concept of a fractal is most often related with geometrical objects satisfying the criteria of self-similarity. Self-similarity means that an object is composed of sub-units and sub-sub-units on multiple levels that statistically resemble the structure of the whole object. These

Corresponding Author: Jawad K. Ali, Department of Electrical and Electronic Engineering, University of Technology, P.O. Box 35239, Baghdad, Iraq

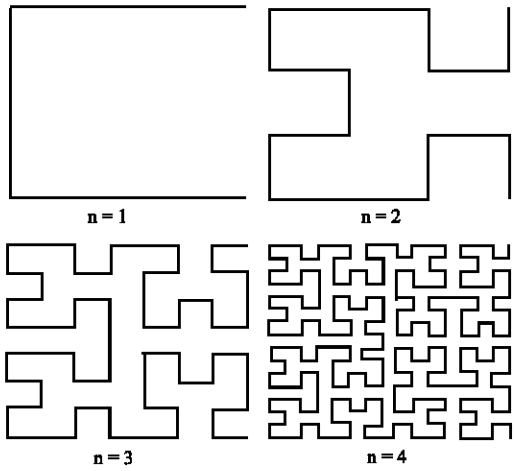

Fig. 2: The first four iteration levels to generate the Hilbert pre-fractal curve

substructures are exactly of the shape as the original but it may be flipped, rotated, or stretched depending on the generation process producing the fractal shape. Figure 1 and 2 demonstrate this property through the generation process of well-known fractal geometries; Peano and Hilbert fractals.

The second concept for a fractal is a fractional dimension. This requirement distinguishes fractals from the Euclidean geometries, which have integer dimensions. The common intuitive idea of dimension is referred to as topological dimension. A point, a line segment, a square and a cube have topological dimensions zero, one, two and three, respectively. This intuitive dimension is always expressed as an integer.

In (Mandelbrot, 1983; Falconer 2003), the Hausdroff-Besicovich dimension is referred to as the fractional dimension and it is defined as, a real number that precisely measures the object's complexity. Mandelbrot defines a fractal as a set for which the Hausdroff-Besicovich dimension strictly exceeds the topological dimension. He refers to this dimension as the fractal dimension of a set. Fractional dimension is related to self-similarity in that; the easiest way to create a figure that has fractional dimension is through self-similarity. The character of non-integer dimension causes the fractal dimension to be useful in measurement, analysis and classification of many fractal shapes, for example, the fractal dimension provides a way to measure how rough fractal curves are. In addition, the fractal dimension can describe how much a fractal curve fills the space.

Fractal structures have found increasing applications in different aspects of science and arts. They are successfully used in the fields of physics, chemistry, biology, architecture, etc… (El-Khamy, 2004).

The research in the field of electrodynamics began soon after the scientists discovered the practical aspects of the fractal geometry. Most efforts had been devoted to understand the physical process and mathematical background of the interaction between electromagnetic waves and fractal structures (Kritikos and Jaggard, 1990; Jaggard, 1995, 1977).

In passive microwave circuits design, such in the design of the different types of filters, fractals have been used widely and extraordinary results were obtained. The space-filling property of fractals had led to producing miniaturized sizes of passive microwave circuits for compact wireless communication systems (Jawad, 2008).

In microwave antenna design, size miniaturization of the normal printed dipole antenna can be accomplished either by the use of high dielectric constant substrates instead of air or some foam materials with dielectric constant nearly like that of air, by the modification of the basic dipole shape, or by a combination of these two techniques (Kumar, 2003). Employing high dielectric constant substrates is the simplest solution, but it exhibits narrow bandwidth, high loss and poor efficiency due to surface wave excitation (Kumar, 2003). Fractals are supposed to be considered in the second category, i.e., antenna shape modification. In this sense, the space-filling property of the fractal antenna offers the required compact size, while its self-similarity makes it resonates in more than one frequency band, due to the many resonating substructures it consists of in the whole structure (Kumar, 2003).

The use of fractals in microwave antenna design has dramatically increased in the recent years, where miniaturized and multiband antennas have to meet the challenges imposed upon the modern communication systems to be compact and multi-functional.

In this study, a new fractal printed GCPW-fed monopole antenna based on tent transformation has been presented for use in modern compact and multi-function communication systems. The adopted feeding technique used will facilitate its integration with MMIC circuits. The proposed antenna dimensions can be scaled to meet the requirements of the compact size and radiation characteristics for the specified applications. Up to the author's knowledge, the only published work about the use of tent fractal geometry in the antenna design is that of Hodlmayr (2004). In that research, a wire dipole antenna has been designed and at the UHF band. The concentration there is mainly focused on practical aspects of the design more than the analytical details. However, the resulting antenna performance seems attractive and encourages antenna designers to start limited but promising research work on the application of this fractal geometry on antenna design (Jawad, 2008).

FRACTAL DIPOLE AND MONOPOLE ANTENNAS

Since, the application of the fractal concept on electrodynamics, much work has been devoted to antenna design (Puente *et al*., 1998; Vinoy *et al*., 2001; Gianvittorio and Samii, 2002; Konstantatos *et al*., 2004; Zhu, 2004; Haji-Hashemi *et al*., 2006; Song *et al*., 2004; Azaro *et al*., 2005; Tahir, 2007). The first reported small fractal antenna is the Koch dipole (Puente *et al*., 1998;. In this research, some of the classical features such bandwidth, resonance frequency and radiation resistance had been improved. Later, different fractal geometries, such as Hilbert, Peano, Minkowski, Sierpinski etc..., have been applied to dipole antenna design Vinoy *et al*., 2001; Gianvittorio and Samii, 2002; Konstantatos *et al*., 2004; Zhu, 2004; Haji-Hashemi *et al*., 2006; Song *et al*., 2004; Azaro *et al*., 2005; Tahir, 2007). The reported designs offered astonishing results of antenna performance, whether in the compact size gained or in the multi-resonant behavior they possess. In Fig. 1 and 2, Hilbert and Peano fractal curves up to the fourth iteration level, (n = 4) are depicted, for the sake of comparison with the presented tent curve fractal. These fractals have been widely used in dipole antenna design.

An interesting point of comparison in this context is the total length of the fractal in each iteration level as a function of the side length, L, of the area containing it. This factor acquires its importance from the fact that it mainly determines the lowest resonance frequency of the multi-band fractal dipole and hence the reduction in size gained in comparison with the classical dipole antenna or other fractally designed dipoles.

For the Hilbert fractal curve, the total length, S_n, in the nth order generation level is given in (Vinoy *et al*., 2001) by:

$$S_n = (2^n + 1)L \quad (1)$$

where, L is the side length.

While, for the Peano fractal curve, the total length, S_n is given by (Zhu *et al*., 2004)as:

$$S_n = (3^n + 1)L \quad (2)$$

where, S_n, n and L are as defined earlier.

It is obvious from Eq. 1 and 2 that, the total length of the curve offered by Peano fractal is greater than that offered by Hilbert fractal of the same generation order with the same side length. This means that Peano fractal curve presents better antenna miniaturization than Hilbert fractal does, when it is used in the design of a fractal dipole.

GENERATION OF FRACTAL TENT TRANSFORMATION

The generation process of the fractal curve based on tent transformations is more complicated than those of both Hilbert and Peano fractals.

The presented fractal curve is constructed by applying geometrical transformations of a unit square with a side length L, representing the well-known tent function, Fig. 3a using the transformation algorithm, which is called multiple reduction copy machine (MRCM) as proposed by (Peitgen *et al*., 2004). This MRCM provides a good metaphor for what is known as deterministic iterated function systems (IFS) in mathematics. The MRCM generates a dynamical iterated function system (IFS), Fig. 3b, (Peitgen *et al*., 2004). Using such an IFS, it is possible to produce a generation level in which all line segments join up to form a single path. As it is clear from Fig. 3b, the IFS constructs such a curve with five transformations and

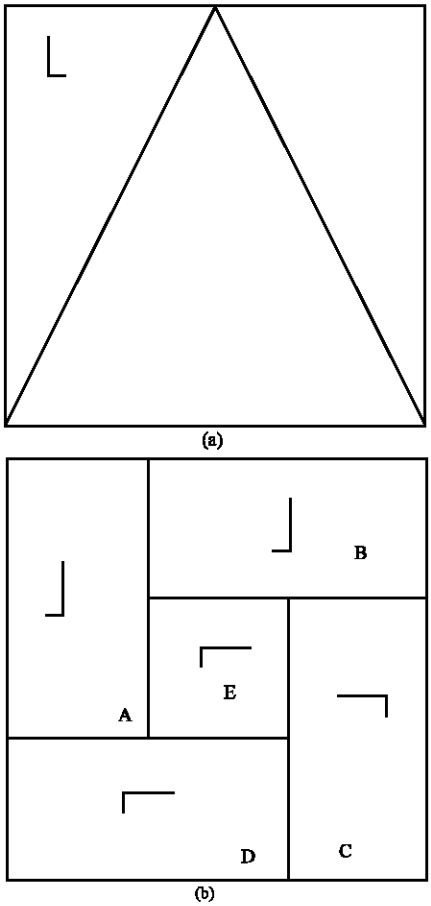

Fig. 3a: The starting tent function as the initiator structure and (b) the iteration function system used to generate the tent fractal curve at the different iteration levels (Peitgen *et al*., 2004)

Table 1: Summary of steps to generate a fractal tent transformation

Step	Width stretched by	Height stretched by	Flipping	Rotati-on (deg.)
A	2/3	1/3	horizontal	none
B	1/3	2/3	horizontal	none
C	1/3	2/3	horizontal	90
D	2/3	1/3	none	-90
E	2/3	2/3	none	-90

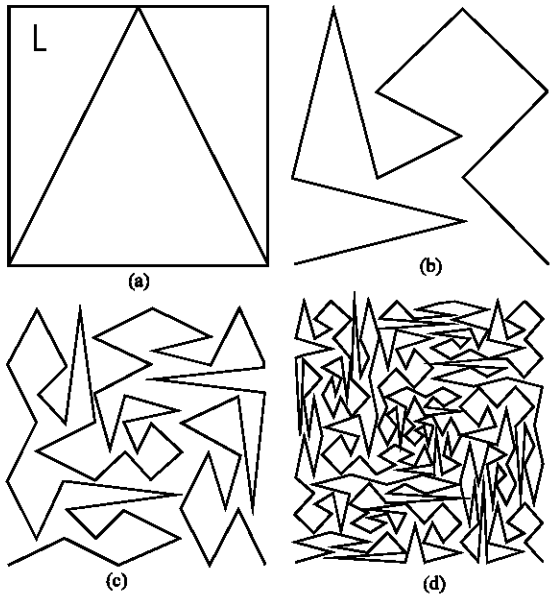

Fig. 4: The details of the generation steps of the tent fractal curves. Structures from (b) to (d) correspond to the first three generation levels

the space-filling property follows from the invariance of the initial square, the tent function, under the IFS. These five transformations, labeled as A, B, C, D and E, which produce any fractal level from its preceding one, are summarized in Table 1. In each transformation, more than one operation has to be performed on the original tent function, such stretching, flipping and/or rotation. Figure (4a-d) show the details of the fractal curves generation process up to the 3rd order (n = 3).

As shown in Fig. 4a-d, the constructed curve in a certain generation level (n) is simply a collage of the five transformations of the previous level (n - 1). Because the initial tent function has a suitable symmetry, one can easily be misled when applying the IFS. The IFS uses the unit square with the inscribed letter L as an indication of the orientation as the initial square, Fig. 3a.

It has been found that the total length S_n, of the tent fractal curve at the nth generation, is:

$$S_n = (\frac{7}{3})^n A_n L \quad (3)$$

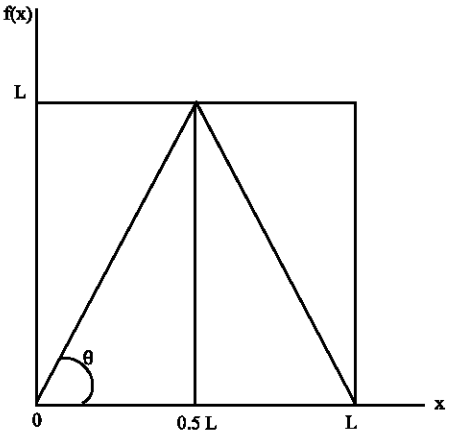

Fig. 5: The tent function with side length, L and a starting angle, θ = 63.435°

where A_n is a constant depending on the starting angle θ, of the initial tent function.

However, the value of this angle is bounded by an upper limit of θ = 63.435°; at which all the vertices of the triangle touches the square, as shown in Fig. 5 and a lower limit of θ = 0°, at which the tent function is considered as a straight line of length equals to the side length, L of the square containing it.

From Fig. 5, the tent function can be described as:

$$f(x) = \begin{cases} ax, & x \le 0.5L \\ a(1-x), & x > 0.5L \end{cases} \quad (4)$$

and the angle θ is defined as:

$$\theta = \tan^{-1} a$$

thus:

$$0^\circ \le \theta \le 63.435^\circ$$

for which:

$$0 \le a \le L$$

It has also been found that A_n, in Eq. 3, is varied as:

$$1 \le A_n \le 2.236$$

for:

$$0^\circ \le \theta \le 63.435^\circ$$

It is worth to note here, that for θ = 63.435°, the tent curve has no longer be a fractal after the 2nd generation

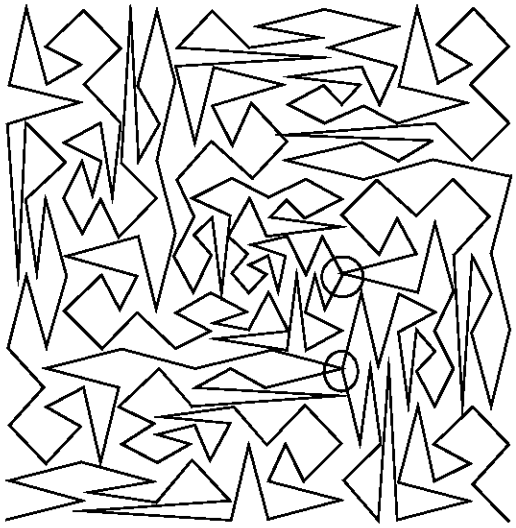

Fig. 6: An enlarged copy of Fig. 4d. The 2 circles shown indicate that, at the 3rd iteration level the resulting structure is not a fractal anymore, since, 2 same points in space have been visited twice

step, since at the 3rd generation step the resulting curve is not self-avoiding . Figure 6 shows an enlarged copy of Fig. 4d. The two circles indicate that the same two points in the space have been visited twice. Nevertheless, the fractal curve can be used at this value of θ, up to the 2nd generation, since a maximum space-filling is gained according to Eq. 3 and it is still self-avoiding.

Practically, if fractal curves are applied, few numbers of iterations are enough to model an antenna (Cohen, 2005; Gianvittorio and Rahmat-Samii, 2002; Haji-Hashemi *et al*., 2006). However, to generate a tent fractal self-avoiding curve with higher generation levels, the starting angle must be reduced.

ANTENNA DESIGN

As a starting step, a monopole antenna based on the 1st iteration, has been modeled using a side length of 13 mm. This will result in a monopole length is of about 67.64 mm. The monopole trace width to length ratio W/S is of about 0.05%, with a trace width of 0.9 mm. This ratio seems practical in most printed dipole and monopole antenna designs reported in the literature (Konstantatos *et al*., 2004; Dubost, 1981). The monopole antenna is supposed to be printed in free space and is fed by grounded coplanar waveguide, GCPW. It has been found that, with GCPW feed, an impedance matching can be maintained over a wide frequency range. In addition, impedance matching has not affected remarkably when scaling the antenna up or down, with its feed. However, it has been verified that the GCPW feed, as the CPW feed, to be an efficient technique to enhance the bandwidth of patch antennas (Haji-Hashemi *et al*., 2006; Liang *et al*., 2005). Each section of the ground plane has a dimension of 11.25×4.2 mm, the width of the center feed strip is of 0.9 mm and the gap between the feed strip and each of the ground plane section has a width of 0.15 mm. The overall height of the resulting monopole, including the GCPW feed, is of 22.35 mm. The monopole is supposed to be printed on a material with a relative dielectric constant of nearly one, or just built in free space. This will directly permit frequency scaling of the modeled monopole to make it resonating at any desired frequency, since material scaling throughout a wide frequency range is not an easy task. Using the same side length of 13 mm, a 2nd iteration monopole antenna has also been modeled and simulated. The resulting monopole antenna length in this case is about 158.26 mm. The monopole trace width to length ratio W/S has been maintained as previously depicted. A proper modification of the GCPW feed dimensions has to be carried out to maintain the required impedance matching.

ANTENNA PERFORMANCE EVALUATION

Many fractal monopole antenna structures based on the 1st and 2nd iterations has been modeled and simulated using a method of moment (MoM) based EM simulator; IE3D from Zeland Software Inc. Figure 7 shows the modeled monopole antennas layout with respect to the coordinate system. Depicted in Fig. 8, the return loss, $S_{11,}$ response of the 1st iteration monopole antenna, where the multi-resonant behavior is very clear. There are three different resonant frequencies, for which ($S_{11} \leq$ -10dB) with reasonable bandwidths around each. These frequencies are located at 4.51, 14.70 and 21.07 GHz, respectively, throughout a swept frequency range from 1 to 30 GHz. This does not prevent the possibility of the existence of other resonating frequencies out of this frequency range. Electric field E_θ elevation pattern directivity display of this monopole antenna, at the first resonant frequency, is shown in Fig. 9. It is worth to note here, that resonating bandwidths achieved in this work are considerably larger than those reported in (Hödlmayr, 2004), due to the use of the GCPW feed.

Other GCPW-fed monopole antennas with different side lengths, L has been modeled and simulated, in an attempt to make a direct relation between the antenna characteristics and its geometrical properties. The simulation swept frequency range has been scaled in proportion for convenience. An interesting result, in this context, has been derived to correlate the GCPW-fed

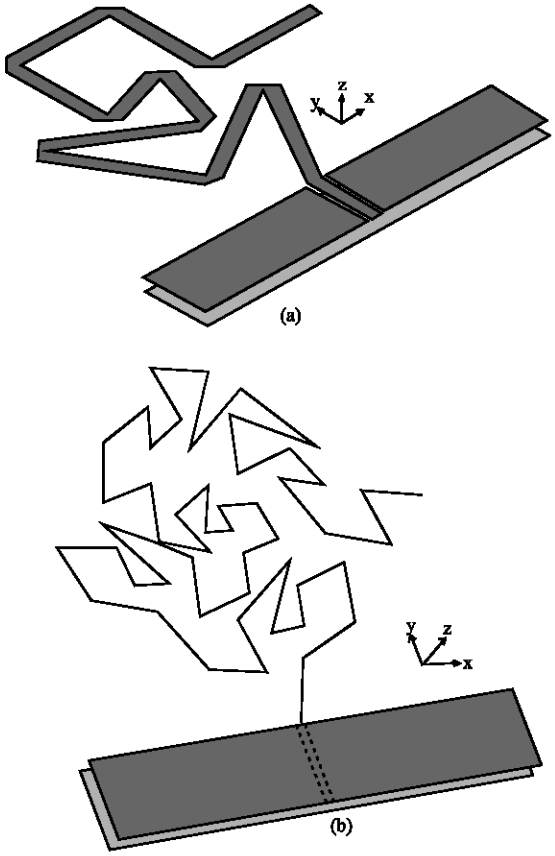

Fig. 7: The layouts of (a) 1st iteration and (b) 2nd iteration fractal monopoles with respect to the coordinate system

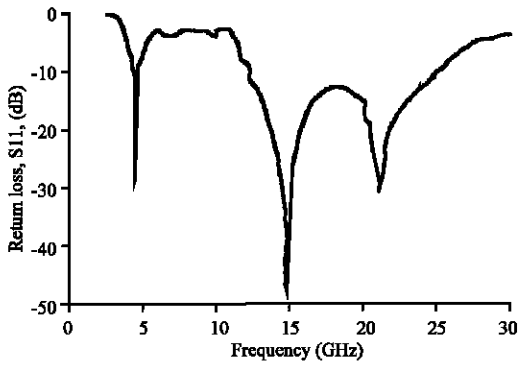

Fig. 8: Return loss response of a 1st iteration monopole with side length of 13 mm

fractal monopole antenna side length, L, with its resonant frequencies. It has been found that the 1st resonant frequency f_{o1}, in GHz, can be approximately determined as:

$$f_{o1} = \frac{58.5}{L} \quad (5)$$

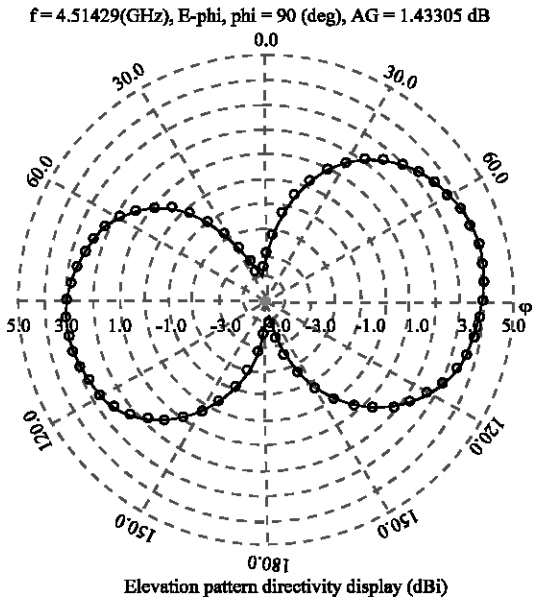

Fig. 9: Electric field E_φ elevation pattern directivity display of a 1st iteration monopole with side length of 13 mm at the first resonant frequency

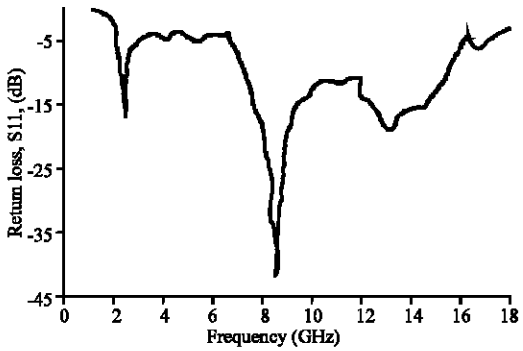

Fig. 10: Return loss response of a 1st iteration monopole with side length of 23.88 mm

where, L is the monopole side length, in mm. Being locating the 1st resonant frequency, the other two resonant frequencies, f_{o2} and f_{o3} can be determined, with less precision, as:

$$f_{o2} \approx 3.3 f_{o1} \quad (6)$$

and

$$f_{o3} \approx 4.8 f_{o1} \quad (7)$$

As an example, to design a GCPW-fed fractal monopole antenna, of the type presented in this research,

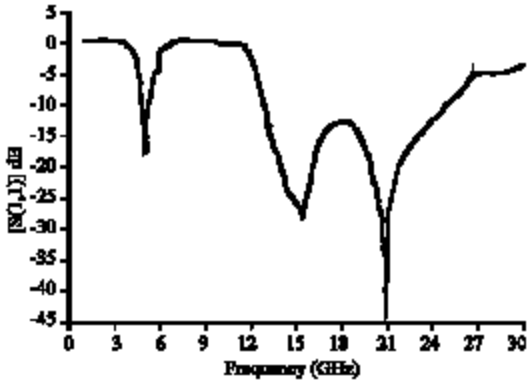

Fig. 11: Return loss response of a 2nd iteration monopole with side length of 13 mm

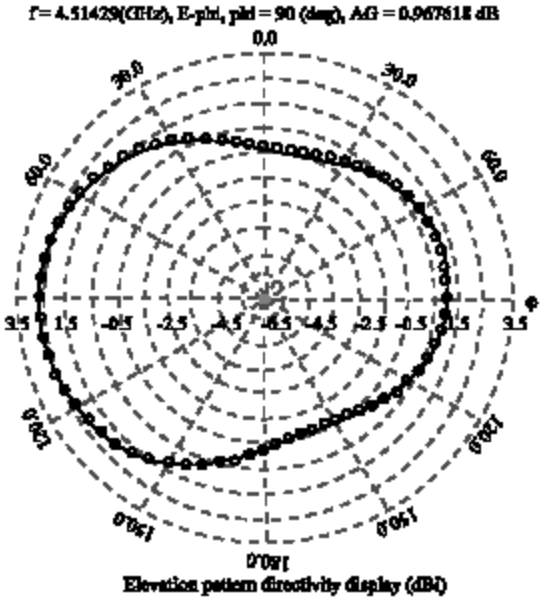

Fig. 12: Electric field E_ϕ elevation pattern directivity display of a 2nd iteration monopole with side length of 13 mm at the first resonant frequency

with the 1st resonance to be located at a frequency of 2.45 GHz, it follows, from Eq. (5) that L will equal to 23.88 mm. The simulated return loss response of this GCPW-fed monopole antenna is shown in Fig. 10. As shown in this figure, the three resonances take place at frequencies of 2.43, 8.47 and 13.11 GHz, respectively, which are near the predictions of Eq. 5-7. These relations can be helpful in the initial design stage. However, a slight dimension tuning might be required for the final design.

Simulation results of the return loss of the 2nd iteration based monopole antennas have shown an interesting point to be discussed (Fig. 11). It has been

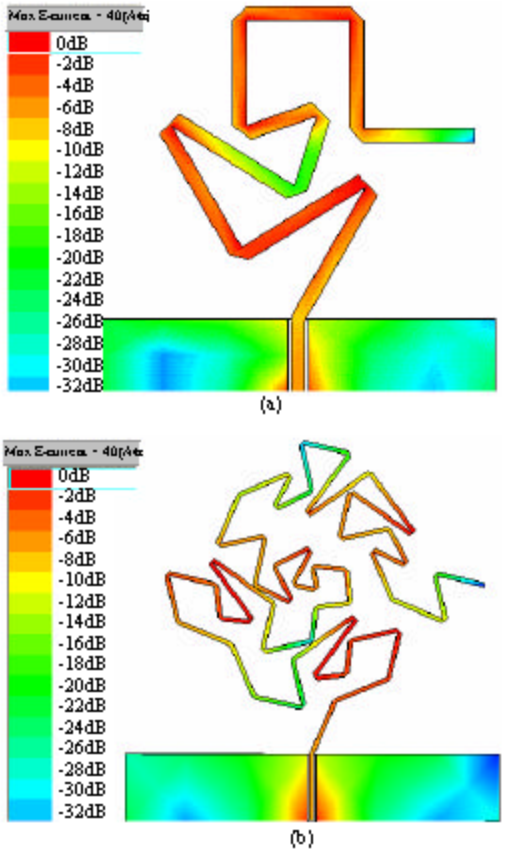

Fig. 13: The current density distributions of (a) 1st iteration monopole antenna and (b) 2nd iteration monopole antenna, with L = 13 mm, at the first resonance frequency

noticed that this response has approximately the same resonance frequencies as those for the 1st iteration monopole of the same side length L (Fig. 12). This well agrees with Hödlmayr (2004) findings.

The only reasonable explanation of this behavior is that, the effective resonating segment lengths in the two monopoles are physically equivalent at the corresponding resonant frequencies; yielding as a consequence similar responses. This fact can partially be assured when investigating the current distributions of a 2 monopoles with different iterations but with the same side length at the same resonance frequency. Figure 13 shows the current density distributions of the previously depicted monopoles with a side length of 13 mm. Careful measurement of the lengths with the highest current densities of these monopoles has shown that their sum, in the two cases, is nearly the same. This issue can similarly be justified for the other resonances.

However, it is expected that a considerable degree of freedom can be provided to antenna designer through the variation of the initial tent starting angle θ, in stead of experiencing higher complex shaped iterations. In such a case, for a certain side length L, it expected to obtain different sets of resonance frequencies corresponding to the different values of θ.

CONCLUSION

A GCPW-fed fractal printed monopole antenna has been presented as a new multiband antenna for use in the multi-functions communication systems. The novel feeding used, has proven to be an attractive technique in maintaining a broad impedance matching throughout a wide frequency range, besides the bandwidth enhancement around the resonant frequencies.

Simulation results of two GCPW-fed monopole antennas based on the 1st and 2nd iterations fractal tent transformations assure the multiband behavior of these antennas. A direct relation has been made between the antenna characteristics and its geometrical properties in an attempt to provide a reliable starting point in the initial design stage. Results showed that the modeled monopole antennas have reasonable antenna parameters at the different resonant frequencies. This makes the proposed antennas promising to be used in multi-function communication systems due to its reasonable multiband response. Additional work has to be carried out to explore the features might be offered by this antenna when varying the starting angle θ of the initial tent function. It is expected to obtain a variety of multi-resonance responses for any given side length L, providing the antenna designer with more degree of freedom.

REFERENCES

Azaro, R., G. Boato, M. Donelli, A. Massa and E. Zeni, 2005. Design of a Pre-Fractal Monopolar Antenna for 3.4-3.6 GHz WI-MAX Band Portable Devices, Technical Report DIT-05-057, University of Trento.

Cohen, N., 2005. Fractal's New Era in Military Antennas, J. RF Design, pp: 12-17.

Dubost, D., 1981. Flat Radiating Dipoles and Applications to Arrays. Research Studies Press, John Wiley and Sons Ltd.

El-Khamy, S.E., 2004. New Trends in Wireless Multimedia Communications Based on Chaos and Fractals. 21st National Radio Sci. Conf. (NRSC2004), pp: INV1 1 -25.

Falconer, K., 2003. Fractal Geometry; Mathematical Foundations and Applications. 2nd Edn., John Wiley and Sons Ltd.

Gianvittorio, J.P. and Y. Rahmat-Samii, 2002. Fractal Antennas: A Novel Miniaturization Technique and Applications. IEEE Antennas and Propagation Magazine, 44 (1): 20-36.

Haji-Hashemi, M.R., H. Mir-Mohammad Sadeghi and V.M. Moghtadai, 2006. Space-filling Patch Antennas with CPW Feed. Progress in Electromagnetics Research Symposium, Cambridge, USA, pp: 26-29.

Hödlmayr, W., 2004. Fractal Antennas. AntenneX, Online Issue no. 81.

Jaggard, D.L., 1977. Fractal electrodynamics: From super Antennas to super lattices. Fractals in engineering: from theory to industrial applications, Springer, London.

Jaggard, D.L., 1995. Fractal Electrodynamics: Wave Interactions with Discretely Self-Similar Structures. In: Electromagnetic Symmetry, Baum C. and H. Kritikos (Eds.). Taylor and Francis Publishers.

Jawad K. Ali, 2008. A New Fractal Printed Dipole Antenna Based on Tent Transformations for Wireless Communication Applications. Accepted for publication at the 2nd Al-Khwarizmi Engineering Conference, University of Baghdad, Baghdad, Iraq.

Jawad K. Ali, 2008. A New Miniaturized Fractal Bandpass Filter Based on Dual-Mode Microstrip Square Ring Resonator. Accepted for publication at the 5th International Multi-Conference on Signals, Systems and Devices, IEEE SSD'08 Conference, Amman, Jordan.

Konstantatos, G., C. Soras, G. Tsachtsiris, M. Karaboikis and V. Makios, 2004. Finite Element Modeling of Minkowski Monopole Antennas Printed on Wireless Devices. Electromagnetics, Taylor and Francis, EMG13571, pp: 1-13.

Kritikos, H.N. and D.L. Jaggard, 1990. Recent Advances in Electromagnetic Theory: On Fractal Electrodynamics. Springer-Verlag, New York.

Kumar, G., 2003. Broadband Microstrip Antennas. Artech House, Inc.

Liang, J., L. Guo, C. Chiau and X. Chen, 2005. CPW-Fed Circular Disc Monopole Antenna for UWB Applications. IEEE Workshop on Antenna Technology, Small Antennas and Novel Metamaterials (IWAT2005), Singapore.

Mandelbrot, B.B., 1983. The fractal Geometry of Nature. W.H. Freeman and Company.

Peitgen, H., H. Jürgens, D. Saupe, 2004. Chaos and Fractals. New Frontiers of Science. 2nd Edn. Springer-Verlag New York.

Puente, C., J. Romeu, R. Pous, J. Ramis and A. Hijazo, 1998. Small But Long Koch Fractal Monopole. Electronic Letters, (38) 1.

Song, C.T.P., P.S. Hall and H. Ghafouri-Shiraz, 2004. Shorted Fractal Sierpinski Monopole Antenna. IEEE Trans. Antennas and Propagat., 52 (10): 2564-2570.

Tahir, M.K., Combined Fractal Dipole Wire Antenna. Loughborough Antennas and Propagation Conference, Loughborough, UK, pp: 65-68.

Vinoy, K.J., K.A. Jose, V.K. Varadan and V.V. Varadan, 2001. Hilbert curve fractal antenna: A small resonant antenna for VHF/UHF applications. Microwave Opt. Technol. Lett., 29 (4): 215-219.

Vinoy, K.J., K.A. Jose, V.K. Varadan and V.V. Varadan, 2001. Resonant frequency of Hilbert curve fractal antennas. In: Proc. Dig. 2001 IEEE AP-S Int. Symp., Boston, MA, pp: 648-652.

Zhu, J., A. Hoorfar and N. Engheta, 2004. Peano Antennas. IEEE Antennas Wireless Propagat. Lett., 3: 71-74.